

# Fractals and Cancer<sup>1</sup>

James W. Baish and Rakesh K. Jain<sup>2</sup>

Department of Mechanical Engineering, Bucknell University, Lewisburg, Pennsylvania 17837 [J. W. B.], and Edwin L. Steele Laboratory, Department of Radiation Oncology, Massachusetts General Hospital, Harvard Medical School, Boston, Massachusetts 02114 [R. K. J.]

## Abstract

Recent studies have shown that fractal geometry, a vocabulary of irregular shapes, can be useful for describing the pathological architecture of tumors and, perhaps more surprisingly, for yielding insights into the mechanisms of tumor growth and angiogenesis that complement those obtained by modern molecular methods. This article outlines the basic methods of fractal geometry and discusses the value and limitations of applying this new tool to cancer research.

## Introduction

Few of us have escaped the ubiquitous fractals that appear on screen savers or coffee table picture books, but what bearing do these unusual and beautiful mathematical fantasies have on tumor architecture? Cancer is often characterized as a chaotic, poorly regulated growth. Not surprisingly, the irregular shapes of cancerous cells, tumors, and vasculature defy description by traditional Euclidean geometry, which is based on smooth shapes such as the line, plane, cylinder, and sphere. In contrast, fractal geometry reveals how an object with irregularities of many sizes may be described by examining how the number of features of one size is related to the number of similarly shaped features of other sizes. By focusing on the irregularity of tumor growth rather than on a single measure of size such as diameter or volume, fractal geometry is well suited to quantify those morphological characteristics that pathologists have long used in a qualitative sense to describe malignancies—their ragged border with the host tissue and their seemingly random patterns of vascular growth.

Before beginning a discussion of applications to cancer, some background on the meaning of “fractal” is in order. Derived from the Latin *fractus* meaning fragmented, a fractal is a mathematical object with a fractional (non-integer) dimension (1). The notion of a dimension other than the familiar, integer possibilities of 1 for a curve, 2 for a surface, and 3 for a solid may seem bizarre, but the extension is quite natural. We typically expect that the number of boxes needed to cover a surface will increase when smaller boxes are used. For most planar objects, we expect that if boxes one-third of their original width are used, then the number of boxes needed to cover the object ( $N$ ) will be nine times greater [that is, three raised to the power two ( $3^2$ )] or, stated in equation form,  $N \propto L^{-2}$ , where  $L$  is the box width. We recognize the power 2 as the dimension of the object. If, instead of a simple, compact object, we count how many boxes are needed to cover the fractal shown in Fig. 1A, we see that each time the box size is reduced by one-third, we need eight (not the expected nine) times as many boxes (Fig. 1B). That is, the number of boxes grows slowly with an

exponent between 1 and 2 according to  $N \propto L^{-D}$ . In this case, we find a non-integer or fractal dimension ( $D = \log(8)/\log(1/3) \cong 1.89$ ).

To satisfy strict mathematical definitions of a fractal, such scaling must apply exactly down to an infinitesimal scale. But as is often the case, naturally occurring objects can only approximate mathematical idealizations. It is common practice to call natural objects “fractals” if they are statistically similar to themselves on magnification over a finite range of length scales (see Appendix A for an illustration from an image-processing technique). Some have argued that self-similarity over only a limited range is insufficient to justify the use of the term “fractal” (2). Although such criticism cannot be lightly disregarded, it seems reasonable to cautiously use fractals as models of natural objects in the same way as a perfect circle might be used to represent the cross section of an artery—with full knowledge that the model is approximate.

With the preceding caveats in mind, this article will describe the application of approximate fractals to cancer as morphometric tools for diagnostic and prognostic purposes and the use of a family of fractal-producing mathematical models known as statistical growth processes (defined in Appendix B) that can mimic tumor and vascular growth. When coupled with traditional models of transport, these newer fractal methods also give insights into tumor morphology and function that can be useful for understanding the movement of imaging tracers in tumors and for the design and delivery of blood-borne treatment modalities.

## Fractal Morphometry Applied to Tumors

Despite the amazing growth in our understanding of the molecular mechanisms of cancer, most diagnosis is still done by visual examination of radiological images, microscopy of biopsy specimens, direct observation of tissues, and so on. These views are typically interpreted in a qualitative manner by clinicians trained to classify abnormal features such as structural irregularities or high indices of mitosis. A more quantitative and hopefully more reproducible approach, which may serve as a useful adjunct to trained observers, is to analyze images with computational tools. Herein lies the potential of fractal analysis as a morphometric measure of the irregular structures typical of tumor growth.

Several comprehensive reviews of the use of fractal dimensions in pathology have recently appeared in the literature (3–6). There is a growing literature that shows fractals to be useful measures of the pathologies of the vascular architecture, tumor/parenchymal border, and cellular/nuclear morphology.

**Tumor Vasculature.** Tumor vasculature has long been known to be more chaotic in appearance than normal vasculature (Fig. 2). Now that angiogenesis has been identified as a critical event in tumor progression and as a potential target for treatment (7), there is an increasing need to understand the origins and consequences of the abnormal vascular architectures found in tumors. Fractals show promise as useful measures of these complex structures.

The best known studies of fractal analysis of healthy and pathological vascular patterns are those of the eye, in which the vasculature

Received 10/19/99; accepted 5/8/00.

The costs of publication of this article were defrayed in part by the payment of page charges. This article must therefore be hereby marked *advertisement* in accordance with 18 U.S.C. Section 1734 solely to indicate this fact.

<sup>1</sup> Supported by National Cancer Institute Grants R15-CA/OD74366 (to J. W. B.) and R35-CA-56591 (to R. K. J.).

<sup>2</sup> To whom requests for reprints should be addressed, at Department of Radiation Oncology, Massachusetts General Hospital, Boston, MA 02114. Phone: (617) 726-4083; Fax: (617) 726-4172; E-mail: jain@steele.mgh.harvard.edu.

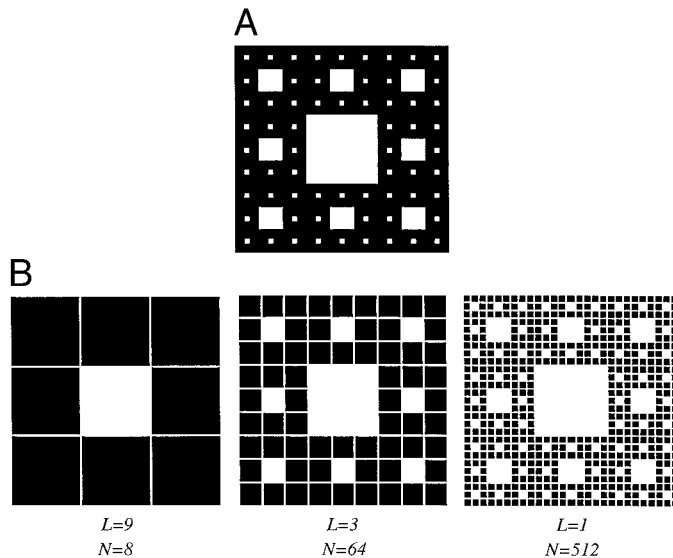


Fig. 1. A, Sierpinski carpet; B, coverage of Sierpinski carpet by boxes of decreasing size.

is readily observed (8–14). To date, detailed images of growing tumor vasculature are not yet available for routine clinical use, but in experimental settings, the vasculature may be directly observed. In our own studies with planar tissue preparations in mice, we have found remarkably consistent scaling exponents (fractal dimensions) for tumor vasculature even among tumor lines that have quite different vascular densities and growth characteristics. Furthermore, these dimensions reveal important aspects of the underlying mechanisms of vascular growth in tumors (15–17). We find that tumor vessels yield dimensions of  $1.89 \pm 0.04$ , whereas normal arteries and veins yield dimensions of  $1.70 \pm 0.03$ , and normal capillaries produce essentially two-dimensional patterns (they are distributed uniformly enough to ensure adequate oxygen throughout the tissue; Ref. 16). We also considered an important secondary measure, the minimum path dimension, that is calculated by the same algorithms but applied to the shortest connected pathway across the image. This yielded values indistinguishable from one for both categories of normal vessels, but a value of  $1.10 \pm 0.04$  for the tumor vessels (16). We find that tumor vessels have a profound sort of tortuosity, with many smaller bends upon each larger bend.

Somewhat different fractal measures (power-law behavior of the Fourier spectrum of gray-scale images) were used by Heymans *et al.* (18) to characterize the microvasculature in cutaneous melanoma. Here too, the fractal dimension quantified the degree of randomness to the vascular distribution, a characteristic not easily captured by the vascular density.

The observed fractal dimensions of the tumor vasculature as a whole and of the minimum path closely correspond to those produced by a statistical growth process known as invasion percolation (see Appendix B). In everyday language, percolation is associated with the movement of water through the random fissures in soil or coffee grounds. In a more technical sense, invasion percolation is an algorithm that models the expansion of a network throughout a medium with randomly distributed heterogeneities in strength. The resulting networks always expand into the weakest available sites, yielding structures with voids on a wide range of length scales and pathways that are tortuous over many scales as well. In Gazit *et al.* (16), invasion percolation with a simulated autocrine mechanism was shown to neatly mimic the transition from normal vasculature to the irregular patterns found in tumors.

The association of tumor vasculature with local heterogeneities is surprising because tumor angiogenesis is typically attributed to gradients in diffusible cytokines that can alter the rates of mitosis, migration, differentiation, and apoptosis of endothelial cells (19). Gradients in diffusing materials frequently lead to tree-like DLA<sup>3</sup>-like patterns (see Appendix B) rather than the more random percolation patterns found in tumor vasculature. How can this apparent contradiction be explained? One possibility is that tumors are sufficiently awash in angiogenic factors that orderly gradients have little opportunity to arise. Tumor vasculature is also known to have an autocrine and a paracrine production of cytokines that further obscures the gradients in the angiogenic factors (20, 21). Because the stimulus to grow is widely available, the remaining constraint is the heterogeneity of the growth-supporting matrix. The fractal dimensions of tumor vasculature indicate that the primary determinant of vascular architecture in tumors is randomness in the underlying matrix rather than gradients in the angiogenic factors. Greater attention to the interaction of the endothelial cells with their surrounding extracellular matrix and stromal cells seems to be warranted (22, 23). The recent discovery that fragments of matrix proteins [such as endostatin, which is derived from collagen XVIII (24)] are regulators of angiogenesis lends credence to this mechano-chemical transduction hypothesis.

**Antiangiogenesis.** Targeting tumor vasculature as a means of controlling tumor growth has been a goal for nearly 30 years. With the recent identification of various antiangiogenic substances, this goal seems almost within reach (7, 19, 24). Thus far, most of this research has focused on the molecules involved and used relatively simple morphological measures such as vessel density. Ultimately, we will need more complete knowledge of the architectural changes that occur during vessel regression. We need to know the patterns as well as the number of vessels present if we are to understand the ability of the vessels to carry out basic functions such as nutrient and drug delivery.

Parsons-Wingerter *et al.* (25) showed that basic fibroblast growth factor and angiostatin caused significant changes in the fractal dimension and vascular density of the developing arteries of the quail chorioallantoic membrane. In another recent study, we (15) measured the fractal dimensions during the growth and subsequent regression of a line of androgen-dependent (Shionogi) tumors in mice after removal of the source of androgens. The blood vessels in these tumors not only reduced their density, but fractal analysis showed that they lost their random, percolation-like architecture and returned to a more normal and regular pattern. Their physiological function also returned to normal (26). This raises some interesting questions about antiangiogenic treatment. The goal of antiangiogenic treatment is to suppress the growth of the tumor by reducing or suppressing the proliferation of tumor blood vessels. Our studies point to an intriguing dilemma in this approach. The irregular geometry of tumor blood vessels impedes the uniform transport of drugs to tumor cells, but it also impedes nutrient delivery to tumor cells. Because antiangiogenic treatment might lead to a more normal vascular pattern with improved transport, the possibility exists for improved drug and oxygen delivery but also for enhanced nutrient transport that could lead to faster growth of cancer cells. The balance between these possible outcomes of antiangiogenic treatment is subtle and will best be revealed by a combination of molecular, physiological, and mathematical analyses of the processes involved.

Our recent studies have shown that invasion percolation can be used both to describe the irregular vascular architecture in tumors and to elucidate some of the mechanisms that regulate the numbers of vessels and the patterns of their interconnections. Each week seems to

<sup>3</sup> The abbreviation used is: DLA, diffusion-limited aggregation.

yield new molecular insights into the suppression of pathological vascular growth (therapeutic antiangiogenesis) or the promotion of new vessels where needed (therapeutic angiogenesis; Refs. 7 and 27–29). Unfortunately, despite quite detailed knowledge of the *quantity* of blood vessels that grow or regress in response to a particular molecular stimulus, we have relatively primitive tools for assessing the *quality* of those vessels, that is, their ability to carry out their primary physiological function, efficient transport (30).

## Modeling Physiological Function

### Dynamic Movement of Blood-borne Substances: Imaging Tracers.

Because the vascular architecture of tumors is so fundamentally different from that in healthy tissues, the movement of blood-borne substances such as imaging tracers can also be expected to show differences. Traditional mathematical models of tissue transport assume either regular patterns of parallel and series blood vessels or well-mixed compartments lacking spatial gradients. Neither assumption adequately accounts for the highly variable vascular patterns found in tumors *in vivo*.

We investigated the spatial and temporal aspects of blood-borne materials in tumors using a fractal model that coupled a tracer transport model to a percolation-based flow model (31, 32). The model predicts highly heterogeneous transport in the tumor, which is clinically significant because some “out of the way” regions of tumor may receive low concentrations of tracer. What little tracer is received may arrive significantly later than in most of the tumor but be retained for longer than average. We also found that the elimination of a tracer from a tumor has an unusually prolonged “tail” that reflects the same basic geometric feature: that transport in some parts of the tumor is dominated by regions of relatively stagnant blood flow. Craciunescu *et al.* (33) used dynamic images taken with magnetic resonance imaging to show that the perfusion front of an imaging tracer in a tumor behaves in the same way that a perfusion front is expected to behave in a percolation network (flowing rapidly in places, flowing slowly in others, and not flowing at all elsewhere).

Fine-scale and dynamic, functional imaging techniques hold great promise for the study and diagnosis of pathological conditions. Such promise can best be achieved when a basic understanding of how blood-borne imaging tracers move throughout a tissue is available. The qualitative differences noted between transport in normal and tumor tissues might be constructively exploited to yield new diagnostic imaging modalities.

**Implications for Drug Delivery and Hypoxia.** The association of tumor vascular architecture with percolation processes has important implications for the delivery of therapy to tumors. The same features of non-uniform delivery that may be valuable for distinguishing tumors in images are potentially disastrous for drug delivery. Non-surgical treatment of tumors relies directly or indirectly on the ability of the blood to carry therapeutic agents to the tumor. Whereas this is obviously true for chemotherapy, even ionizing radiation works best in well-oxygenated tumors. Given that tumor vasculature is often expanding rapidly and may have a high vascular density and consist of relatively dilated blood vessels, it may be surprising that drug and oxygen transport to tumors is difficult (34, 35).

Some of the challenges in treating solid tumors with blood-borne substances can be explained by using fractal, percolation-based computer models (17). Simulated percolation processes, like *in vivo* tumors, produce highly variable intervascular distances that leave large regions of the tumor further from the nearest blood vessel than even a freely diffusing substance like oxygen can diffuse (36). High molecular weight drugs, with their associated lower diffusivities, have little chance of reaching all of the tumor cells (34, 35). The recent

theoretical studies of West *et al.* (37) predict that the most efficient transport of materials by an internal network such as the vasculature should have a minimum path dimension of unity. The elevated minimum path dimension found in tumors is therefore consistent with the suboptimal delivery of nutrients and drugs in tumors. Highly heterogeneous networks produced by percolation are known to have a higher resistance to flow than more regular networks (38). This results from the flow being carried in only a few vessels, whereas others carry little or no flow. In fact, some parts of a tumor may be remote from a source of blood-borne substances, even when many blood vessels are nearby. For example, oxyhemoglobin saturations show little correlation with vascular density (39). Percolation networks, like tumors, exhibit regions of stagnant flow and low oxygen levels within blood vessels. Whereas other factors may be in effect, it appears that the apparent paradox that tumors offer a higher resistance to blood flow than normal vascular networks despite having larger diameter vessels and higher vascular densities (40, 41) may have a purely geometrical explanation: percolation networks are not optimally arranged to permit efficient flow.

The suboptimal drug delivery and hypoxia found in tumors are well-known consequences of the morphometry (34, 35, 39, 42–44). Such heterogeneity need not have fractal characteristics to have such effects, but the insights provided by fractal image analysis and the percolation model provide a unifying framework yielding mechanistic explanations for a combination of observations including highly variable intervessel distances, high geometrical resistance to blood flow, hypoxic tissue, low oxygen saturations even within tumor blood vessels, and heterogeneous blood flow. Of course, other molecular processes are also relevant, but when combined with percolation-based models, a fuller picture is revealed.

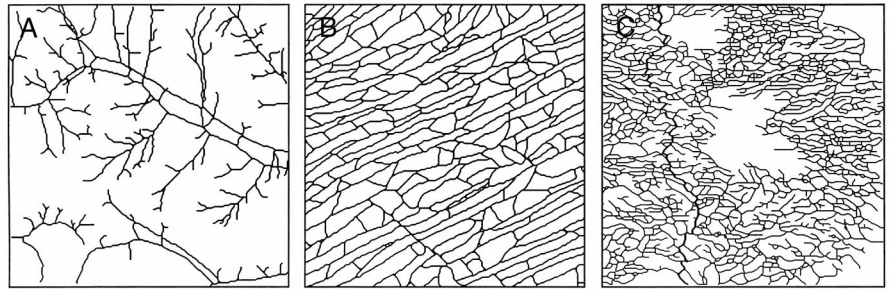
## Future Directions and Conclusions

Pathologists are skilled in examining the epithelial-connective tissue interface that demarcates the border between a tumor and the surrounding healthy tissue. The nature of the tumor border, whether infiltrative and invasive or purely expansive, provides information useful not only for prognosis but also for diagnosis (whether benign or malignant). In a study by Landini and Rippin (45), the epithelial-connective tissue interface of the oral mucosa was examined. The lesions were classified during routine diagnosis into four categories: (a) normal; (b) mild dysplasia; (c) moderate to severe dysplasia; and (d) carcinoma. Fractal image analysis of the lesions subsequently revealed the fractal dimensions and SDs of the four categories were  $1.07 \pm 0.05$ ,  $1.08 \pm 0.09$ ,  $1.16 \pm 0.08$ , and  $1.41 \pm 0.08$ , respectively. Whereas the differences were not sufficiently great to be acceptable as an independent means of diagnosis, they were nonetheless consistent measures of the degree of tortuosity of the interface. Landini and Rippin went on to describe a more sophisticated multifractal analysis that yields a spectrum of fractal values instead of a single value for each image. This method provided a still more reliable discrimination of the pathological state of the tissues. Lefebvre and Benali (46) and Pohlman *et al.* (47) have demonstrated that fractal methods may also be useful for analyzing digitized mammograms, raising hopes that the number of false positive mammograms might be reduced.

Whereas progressively more irregularity, with an associated increase in fractal dimension, is a common observation with tumor growth (47–56), it is by no means a universal result. The distribution of cells in normal bone marrow was found to exhibit a fractal dimension, whereas metastatic lesions of the bone marrow showed a loss of fractal structure indicating a more uniform filling of the tissue space (57). Using a cellular automata model (see Appendix B), Smolle (58) showed that the fractal dimension of the tumor-stromal border de-



Fig. 2. Skeletonized images of vascular networks. A, normal arteries and veins. B, normal subcutaneous capillaries. C, tumor vasculature. The path of minimum length is highlighted on the tumor vasculature to illustrate the tortuosity of these vessels. (Adapted from Ref. 16.)



pended on a complex interplay of tumor cell motility, tumor and stromal proliferation, cohesion, autocrine and paracrine growth stimulation, and tumor and stromal destruction.

Whereas our present discussion has focused on applications of fractal analysis to tumor vasculature and the tumor border, several groups are seeking to extend the use of fractals to the classification of abnormalities of cellular and nuclear structures (5, 59–61). Explanations for why structures at this scale should display changes in fractal dimension under pathological conditions remain to be explored.

Although better understood than cellular morphology, determinants of vascular morphology are just beginning to be revealed by molecular methods (62, 63). The extent to which specific vascular growth factors may be linked to specific vascular morphologies is an area of ongoing study. Hopefully, when molecular methods are combined with fractal analysis and more classical morphometric methods (64), a more complete understanding of tumor pathology may be obtained.

If carefully applied, fractal methods may someday have a significant impact on our understanding of challenges in treatment delivery and diagnosis of cancer. Being able to quantify the irregular structures that are present in tumors helps to clarify why treatment is so frustratingly difficult, a disappointing but important finding. More constructively, the same irregularities that thwart treatment appear to be promising means of highlighting tumors in new imaging procedures based on the patterns of tracer movement. Fractal analysis shows its greatest promise as an objective measure of seemingly random structures and as a tool for examining the mechanistic origins of pathological form. Whether fractals will ultimately find a place in the oncologist's toolbox awaits more controlled comparisons with conventional pathological procedures.

## Acknowledgments

We gratefully acknowledge the insightful comments of Brian Stoll.

## Appendices

**Appendix A: How Is a Fractal Dimension Measured From an Image?** The fractal dimension of an image may be estimated by various techniques: (a) box-counting; (b) correlation; (c) sandbox; (d) Fourier spectrum; and (e) others (65). When applied to images of blood vessels, these methods yield scaling relationships that are statistical best fits to a power-law relationship within a finite range of scales (5). Fig. 3 illustrates the use of a statistical box-counting method (similar to that illustrated in Fig. 1) to estimate the fractal dimension of the path of minimum length from an image of tumor blood vessels (Fig. 2). In the case illustrated, the power-law relationship holds for the range between 3 and 100 pixels or about 1.5 orders of magnitude. Even under the best conditions, the range of fractal scaling in an image cannot extend below the lower limit of the pixel size or above the size of the image as a whole. The empirical concept of an asymptotic fractal has been proposed as a better fit near the limits of power-law behavior and to remove elements of user subjectivity regarding the range over which the fit should be performed (66).

**Appendix B: Statistical Growth Processes.** Statistical growth processes, such as invasion percolation (which is especially useful as a model of tumor

vasculature), comprise a class of mathematical models that allow computer simulation of a variety of dynamic processes that govern the shape and growth of natural objects. The most standard forms of these models use a simple set of rules to define how each "cell" on a regular grid will respond to its immediate or extended neighborhood by growing, dying, migrating, infecting, resisting, or a similar action. The rules in the algorithms may be strictly deterministic, such as "if a living cell has three neighbors, then it will die in the next time step." Alternatively, a random number generator may be used to simulate events that occur with a given probability. Examples include a cell

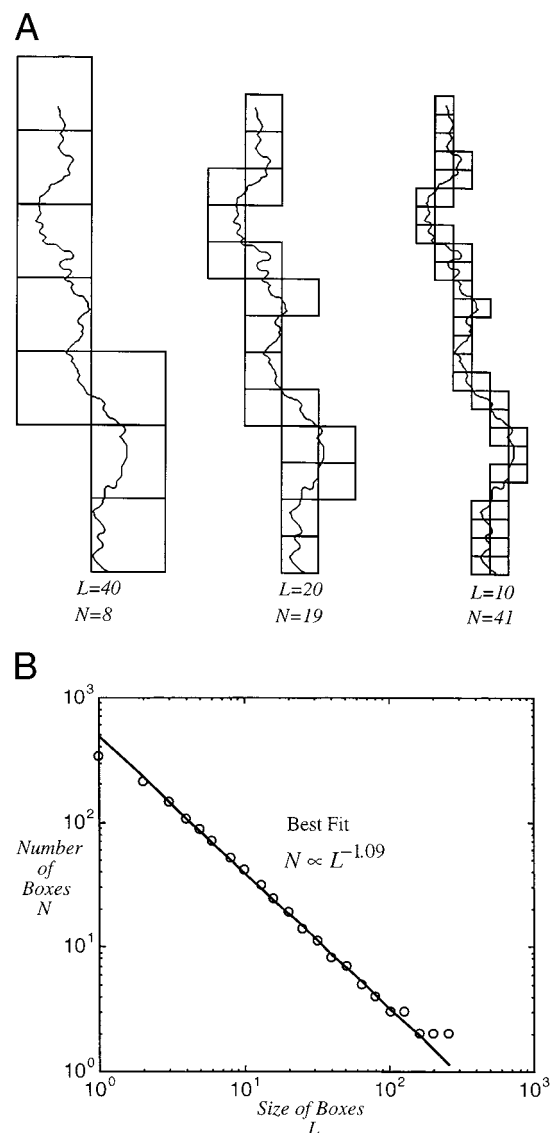


Fig. 3. A, minimum path from tumor vasculature in Fig. 2 covered by boxes of decreasing size. B, best power-law fit of number of boxes to size of boxes.

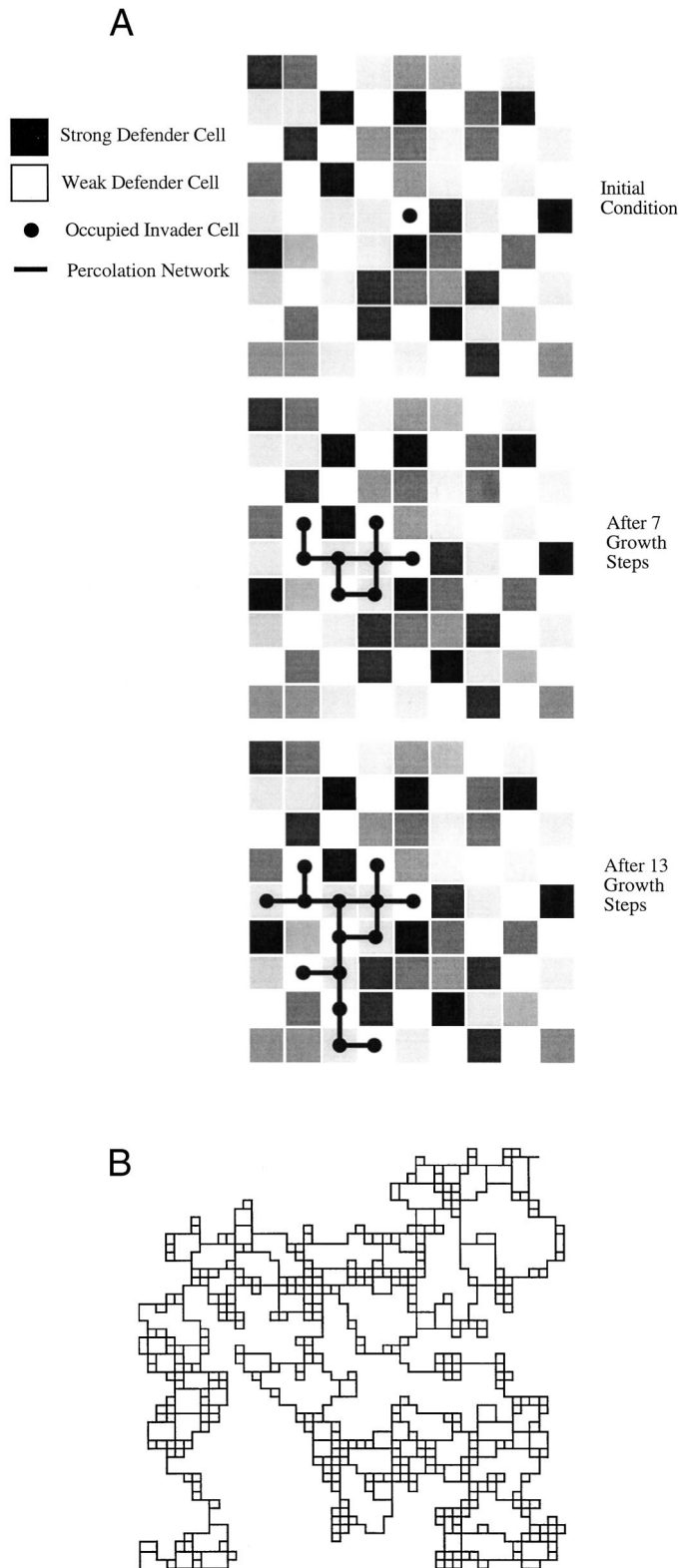


Fig. 4. A, first several steps of an invasion percolation algorithm. B, simulated vascular network created by an invasion percolation algorithm.

that has a 75% probability of dying in the next time step if it has exactly three neighbors and a migrating cell that may move left, right, up, or down with equal likelihood. With the aid of rapid and repeated runs of the program, the investigator may study how parametric changes in the algorithm influence the resulting patterns of activity. The resulting patterns can be simple and stable or

dynamic with regular, random, or fractal shapes. Physicists have shown that the fractal dimensions of the patterns produced by certain simple growth algorithms fall into broad categories known as universality classes (65, 67, 68) with fractal dimensions that are remarkably insensitive to the details of how they are implemented. Descriptions of several well-known algorithms follow.

**Cellular Automata.** Cellular automata constitute a large class of models that produce evolving patterns of cells. Typically, each cell responds at each time step to the presence or absence of cells in their immediate neighborhood. The best known such algorithm is the early computer classic called the game of Life, in which cells die if they are surrounded by less than two or more than four neighbors, and cells are born in empty sites if exactly three of their neighbors are alive. Whereas several types of cellular automata produce growing patterns, most do not lead to fractal shapes.

**Eden Growth.** The simplest statistical growth process, Eden growth, was introduced in 1961. Growth on a planar grid of potential growth sites is initiated at a single "infected" site. The next site to be infected is chosen at random from among the nearest neighbors of the original site. Growth continues by randomly infecting the neighbors of the cluster as it expands. Because the interior of this cluster has been shown to be nearly uniformly occupied, whereas the border is a fractal, the Eden algorithm is appealing as a simple model for the tumor/parenchymal border.

**DLA.** DLA is a statistical growth process that progresses much like Eden growth, but the addition of sites occurs with the highest probability where the gradient of a substance that is diffusing toward the existing cluster is greatest. The sites with the highest gradients tend to occur at the sharpest and outermost points of the cluster, thus leading to the unstable and rapid growth of these points. A dendritic structure results that has been suggested as model of growth for healthy arteries. Unlike cellular automata and Eden growth, DLA is considered a global model as opposed to a local model. Whereas the probability of growth depends on the local gradient, the gradient itself is determined by the patterns of diffusion around the entire cluster that arise from the shape of the cluster as a whole. Growth therefore exhibits long-range correlation, an important characteristic in a structure that may approximate global optimization for transport of metabolic materials. The fractal dimension of a DLA cluster as a whole is known to be about 1.71 in a plane with a minimum path dimension of 1.00 (69, 70).

**Invasion Percolation.** As with Eden growth and DLA, invasion percolation (Fig. 4) begins with a single occupied site on a lattice of potential growth sites. Each potential growth site is initially assigned a random value that may be interpreted as a "strength." Growth proceeds at each time step by expanding into the neighboring site that has the lowest strength. The resulting percolation clusters develop holes of many sizes, leading to a fractal dimension of 1.89 in a plane for the cluster as a whole and a minimum path dimension of 1.13 (71). Such processes are considered locally random because they display no long-range correlation (38, 72).

## References

1. Mandelbrot, B. B. *The Fractal Geometry of Nature*. New York: W. H. Freeman, 1982.
2. Avnir, D., Biham, O., Lidar, D., and Malcai, O. Is the geometry of nature fractal? *Science* (Washington DC), 279: 39–40, 1998.
3. Losa, G. A. Fractals in pathology: are they really useful? *Pathologica*, 87: 310–317, 1995.
4. Cross, S. S. Fractals in pathology. *J. Pathol.*, 182: 1–8, 1997.
5. Coffey, D. S. Self-organization, complexity and chaos: the new biology for medicine. *Nat. Med.*, 4: 882–885, 1998.
6. Landini, G. Pathology in geometry, and geometry in pathology. In: C. A. Pickover (ed.) *Fractal Horizons*, pp. 251–262. New York: St. Martin's Press, 1996.
7. Folkman, J. Tumor angiogenesis. In: J. Mendelsohn, P. M. Howley, M. A. Israel, and L. A. Liotta (eds.), *The Molecular Basis of Cancer*, pp. 206–232. Philadelphia: W. B. Saunders, 1995.
8. Family, F., Masters, B. R., and Platt, D. E. Fractal pattern formation in the human retinal vessels. *Physica D*, 38: 98–103, 1989.
9. Daxer, A. Fractals and retinal vessels. *Lancet*, 339: 618, 1992.
10. Daxer, A. Characterisation of the neovascularisation process in diabetic retinopathy by means of fractal geometry: diagnostic implications. *Graefes Arch. Clin. Exp. Ophthalmol.*, 231: 681–686, 1993.
11. Daxer, A. The fractal geometry of proliferative diabetic retinopathy: implications for the diagnosis and the process of retinal vasculogenesis. *Curr. Eye Res.*, 12: 1103–1109, 1993.
12. Daxer, A., and Ettl, A. Corneal vascularisation and its relation to the physical properties of the tissue: a fractal analysis. *Curr. Eye Res.*, 14: 263–268, 1995.
13. Landini, G., Misson, G. P., and Murray, P. I. Fractal analysis of the normal human retinal fluorescein angiogram. *Curr. Eye Res.*, 12: 23–27, 1993.

14. Mainster, M. A. The fractal properties of retinal vessels: embryological and clinical implications. *Eye (Lond.)*, 4: 235–241, 1990.
15. Gazit, Y., Baish, J. W., Safabakhsh, N., Leunig, M., Baxter, L. T., and Jain, R. K. Fractal characteristics of tumor vascular architecture during tumor growth and regression. *Microcirculation*, 4: 395–402, 1997.
16. Gazit, Y., Berk, D. A., Leunig, M., Baxter, L. T., and Jain, R. K. Scale-invariant behavior and vascular network formation in normal and tumor tissue. *Phys. Rev. Lett.*, 75: 2428–2431, 1995.
17. Baish, J. W., Gazit, Y., Berk, D. A., Nozue, M., Baxter, L. T., and Jain, R. K. Role of tumor network architecture in nutrient and drug delivery: an invasion percolation-based network model. *Microvasc. Res.*, 51: 327–346, 1996.
18. Heymans, O., Blacher, S., Brouers, F., and Pierard, G. E. Fractal quantification of microvasculature heterogeneity in cutaneous melanoma. *Dermatology (Basel)*, 198: 212–217, 1999.
19. Folkman, J. Angiogenesis in breast cancer. In: K. I. Bland and E. M. I. Copeland (eds.), *The Breast: Comprehensive Management of Benign and Malignant Disease*, pp. 586–603. Philadelphia: W. B. Saunders, 1998.
20. Gualandris, A., Rusnati, M., Belleri, M., Nelli, E. E., Bastaki, M., Molinari-Tosatti, M. P., Bonardi, F., Parolini, S., Albini, A., Morbidelli, L., Ziche, M., Corallini, A., Possati, L., Vacca, A., Rabatti, D., and Presta, M. Basic fibroblast growth factor overexpression in endothelial cells: an autocrine mechanism for angiogenesis and angioproliferative diseases. *Cell Growth Differ.*, 7: 147–160, 1996.
21. Helmlinger, G., Endo, M., Ferrera, N., Hlatky, L., and Jain, R. K. Autocrine VEGF promotes endothelial network formation which is proliferation-independent. *Nature (Lond.)*, 405: 139–141, 2000.
22. Stromblad, S., and Cheresh, D. A. Cell adhesion and angiogenesis. *Trends Cell Biol.*, 6: 462–486, 1996.
23. Fukumura, D., Xavier, R., Sugiura, T., Chen, Y., Park, E. C., Lu, N., Selig, M., Nielsen, G., Taksir, T., Jain, R. K., and Seed, B. Tumor induction of VEGF promoter activity in stromal cells. *Cell*, 94: 715–725, 1998.
24. O'Reilly, M. S., Boehm, T., Shing, Y., Fukai, N., Vasios, G., Lane, W. S., Flynn, E., Birkhead, J. R., Olsen, B. R., and Folkman, J. Endostatin: an endogenous inhibitor of angiogenesis and tumor growth. *Cell*, 88: 277–285, 1997.
25. Parsons-Wingter, P., Lwai, B., Yang, M. C., Elliott, K. E., Milaninia, A., Redlitz, A., Clark, J. I., and Sage, E. H. A novel assay of angiogenesis in the quail chorioallantoic membrane: stimulation by bFGF and inhibition by angiostatin according to fractal dimension and grid intersection. *Microvasc. Res.*, 55: 201–214, 1998.
26. Jain, R. K., Safabakhsh, N., Sckell, A., Chen, Y., Jiang, P., Benjamin, L., Yuan, F., and Keshet, E. Endothelial cell death, angiogenesis, and microvascular function following castration in an androgen-dependent tumor: role of vascular endothelial growth factor. *Proc. Natl. Acad. Sci. USA*, 95: 10820–10825, 1998.
27. Hanahan, D., and Folkman, J. Patterns and emerging mechanisms of the angiogenic switch during tumorigenesis. *Cell*, 86: 353–364, 1996.
28. Kerbel, R. S., Vitoria-Petit, A., Okada, F., and Rak, J. Establishing a link between oncogenes and tumor angiogenesis. *Mol. Med.*, 4: 286–295, 1998.
29. Fidler, I. J., Kumar, R., Bielenberg, D. R., and Ellis, L. M. Molecular determinants of angiogenesis in cancer metastasis. *Cancer J. Sci. Am.*, 4: S58–S66, 1998.
30. Jain, R. K., Schlenger, K., Hockel, M., and Yuan, F. Quantitative angiogenesis assays: progress and problems. *Nat. Med.*, 3: 1203–1208, 1997.
31. Baish, J. W., Smith, J. H., Hamberg, L., and Jain, R. K. Spatio-temporal aspects of transport in tumors: a percolation model. *Ann. Biomed. Eng.*, 25: S-7, 1997.
32. Baish, J. W., Zawilski, K., and Jain, R. K. Architectural heterogeneity of tumor vascular networks leads to power-law tracer washout. *Ann. Biomed. Eng.*, 26: S-58, 1998.
33. Craciunescu, O. I., Das, S. K., and Clegg, S. T. Dynamic contrast-enhanced MRI and fractal characteristics of percolation clusters in two-dimensional tumor blood perfusion. *J. Biomech. Eng.*, 121: 480–486, 1999.
34. Jain, R. K. Barriers to drug delivery in solid tumors. *Sci. Am.*, 271: 58–65, 1994.
35. Jain, R. K. The next frontier of molecular medicine: delivery of therapeutics. *Nat. Med.*, 4: 655–657, 1998.
36. Helmlinger, G., Yuan, F., Dellian, M., and Jain, R. K. Interstitial pH and pO<sub>2</sub> gradients in solid tumors *in vivo*: high-resolution measurements reveal a lack of correlation. *Nat. Med.*, 3: 177–182, 1997.
37. West, G. B., Brown, J. H., and Enquist, B. J. The fourth dimension of life: fractal geometry and allometric scaling of organisms. *Science (Washington DC)*, 284: 1677–1679, 1999.
38. Stauffer, D., and Aharony, A. *Introduction to Percolation Theory*, 2nd ed. London: Taylor & Francis, 1992.
39. Fenton, B. M., Rofstad, E. K., Degner, F. L., and Sutherland, R. M. Cryospectrophotometric determination of tumor intravascular oxyhemoglobin saturations: dependence on vascular geometry and tumor growth. *J. Natl. Cancer Inst.*, 80: 1612–1619, 1988.
40. Less, J. R., Skalak, T. C., Sevcick, E. M., and Jain, R. K. Microvascular architecture in mammary carcinoma: branching patterns and vessel dimensions. *Cancer Res.*, 51: 265–273, 1991.
41. Less, J. R., Posner, M. C., Skalak, T. C., Wolmark, N., and Jain, R. K. Geometric resistance and microvascular network architecture in human colon carcinoma. *Microcirculation*, 41: 25–33, 1997.
42. Fenton, B. M., and Way, B. A. Vascular morphometry of KHT and RIF-1 murine sarcomas. *Radiother. Oncol.*, 28: 57–62, 1993.
43. Secomb, T. W., Hsu, R., Dewhirst, M. W., Klitzman, B., and Gross, J. F. Analysis of oxygen transport to tumor tissue by microvascular networks. *Int. J. Radiat. Oncol. Biol. Phys.*, 25: 481–489, 1993.
44. Vaupel, P. Oxygenation of human tumors. *Strahlenther. Onkol.*, 166: 377–386, 1990.
45. Landini, G., and Rippin, J. W. Fractal dimensions of the epithelial-connective tissue interfaces in premalignant and malignant epithelial lesions of the floor of the mouth. *Anal. Quant. Cytol. Histol.*, 15: 144–149, 1993.
46. Lefebvre, F., and Benali, H. A fractal approach to the segmentation of microcalcifications in digital mammograms. *Med. Phys.*, 22: 381–390, 1995.
47. Pohlman, S., Powell, K., Obuchowski, N. A., Chilcote, W. A., and Grundfest-Broniatowski, S. Quantitative classification of breast tumors in digitized mammograms. *Med. Phys.*, 23: 1337–1345, 1996.
48. Byng, J. W., Boyd, N. F., Little, L., Lockwood, G., Fishell, E., Jong, R. A., and Yaffe, M. J. Symmetry of projection in the quantitative analysis of mammographic images. *Eur. J. Cancer Prev.*, 5: 319–327, 1996.
49. Claridge, E., Hall, P. N., Keefe, M., and Allen, J. P. Shape analysis for classification of malignant melanoma. *J. Biomed. Eng.*, 14: 229–234, 1992.
50. Caldwell, C. B., Stapleton, S. J., Holdsworth, D. W., Jong, R. A., Weiser, W. J., Cooke, G., and Yaffe, M. J. Characterisation of mammographic parenchymal pattern by fractal dimension. *Phys. Med. Biol.*, 35: 235–247, 1990.
51. Sedivy, R. Fractal tumours: their real and virtual images. *Wien Klin. Wochenschr.*, 108: 547–551, 1996.
52. Peiss, J., Verlande, M., Ameling, W., and Gunther, R. W. Classification of lung tumors on chest radiographs by fractal texture analysis. *Invest. Radiol.*, 31: 625–629, 1996.
53. Boone, J. M., Lindfors, K. K., Beatty, C. S., and Seibert, J. A. A breast density index for digital mammograms based on radiologists' ranking. *J. Digital Imaging*, 11: 101–115, 1998.
54. Sedivy, R., and Windischberger, C. Fractal analysis of a breast carcinoma: presentation of a modern morphometric method. *Wien. Med. Wochenschr.*, 148: 335–337, 1998.
55. Velanovich, V. Fractal analysis of mammographic lesions: a prospective, blinded trial. *Breast Cancer Res. Treat.*, 49: 245–249, 1998.
56. Waliszewski, P. Distribution of gland-like structures in human gallbladder adenocarcinomas possesses fractal dimension. *J. Surg. Oncol.*, 71: 189–195, 1999.
57. Moatemed, F., Sahimi, M., and Naeim, F. Fractal dimension of the bone marrow in metastatic lesions. *Hum. Pathol.*, 29: 1299–1303, 1998.
58. Smolle, J. Fractal tumor stromal border in a nonequilibrium growth model. *Anal. Quant. Cytol. Histol.*, 20: 7–13, 1998.
59. Irinopoulou, T., Rigaut, J. P., and Benson, M. C. Toward objective prognostic grading of prostatic carcinoma using image analysis. *Anal. Quant. Cytol. Histol.*, 15: 341–344, 1993.
60. Doudkine, A., Macaulay, C., Poulin, N., and Palcic, B. Nuclear texture measurements in image cytometry. *Pathologica*, 87: 286–299, 1995.
61. Losa, G. A., Graber, R., Baumann, G., and Nonnenmacher, T. F. Steroid hormones modify nuclear heterochromatin structure and plasma membrane enzyme of MCF-7 cells. A combined fractal, electron microscopical and enzymatic analysis. *Eur. J. Histochem.*, 42: 21–29, 1998.
62. Metzger, R. J., and Krasnow, M. A. Genetic control of branching morphogenesis. *Science (Washington DC)*, 284: 1635–1639, 1999.
63. Carmeliet, P. Mechanisms of angiogenesis and arteriogenesis. *Nat. Med.*, 6: 389–395, 2000.
64. Perez-Atayde, A. R., Sallan, S. E., Tedrow, U., Connors, S., Allred, E., and Folkman, J. Spectrum of tumor angiogenesis in bone marrow of children with acute lymphoblastic leukemia. *Am. J. Pathol.*, 150: 815–821, 1997.
65. Landini, G. Applications of fractal geometry in pathology. In: P. M. Iannaccone and M. Khokha (eds.), *Fractal Geometry in Biological Systems*, pp. 205–246. Boca Raton, FL: CRC Press, 1996.
66. Rigaut, J. P., Schoevaert-Brossault, D., Downs, A. M., and Landini, G. Asymptotic fractals in the context of grey-scale images. *J. Microsc.*, 189: 57–63, 1998.
67. Vicsek, T. *Fractal Growth Phenomena*, 2nd ed. Singapore: World Scientific, 1992.
68. Stanley, H. E. Fractals and multifractals: the interplay of physics and geometry. In: A. Bunde and S. Havlin (eds.), *Fractals and Disordered Systems*, pp. 1–49. Berlin: Springer-Verlag, 1991.
69. Meakin, P. Diffusion-controlled cluster formation in 2–6 dimensional space. *Phys. Rev. A*, 27: 1495–1507, 1983.
70. Meakin, P., Majid, I., Havlin, S., and Stanley, H. E. Topological properties of diffusion limited aggregation and cluster-cluster aggregation. *J. Phys. A* 17: L975–L981, 1984.
71. Herrmann, H. J., and Stanley, H. E. The fractal dimension of the minimum path in two- and three-dimensional percolation. *J. Phys. A*, 21: L829–L833, 1988.
72. Sahimi, M. *Applications of Percolation Theory*. London: Taylor and Francis, 1994.

# Cancer Research

The Journal of Cancer Research (1916–1930) | The American Journal of Cancer (1931–1940)

**AACR** American Association  
for Cancer Research

## Fractals and Cancer

James W. Baish and Rakesh K. Jain

*Cancer Res* 2000;60:3683-3688.

**Updated version** Access the most recent version of this article at:  
<http://cancerres.aacrjournals.org/content/60/14/3683>

**Cited articles** This article cites 58 articles, 6 of which you can access for free at:  
<http://cancerres.aacrjournals.org/content/60/14/3683.full#ref-list-1>

**Citing articles** This article has been cited by 23 HighWire-hosted articles. Access the articles at:  
<http://cancerres.aacrjournals.org/content/60/14/3683.full#related-urls>

**E-mail alerts** [Sign up to receive free email-alerts](#) related to this article or journal.

**Reprints and Subscriptions** To order reprints of this article or to subscribe to the journal, contact the AACR Publications Department at [pubs@aacr.org](mailto:pubs@aacr.org).

**Permissions** To request permission to re-use all or part of this article, use this link  
<http://cancerres.aacrjournals.org/content/60/14/3683>.  
Click on "Request Permissions" which will take you to the Copyright Clearance Center's (CCC) Rightslink site.